The Impact of Pacific SSTA on the Interannual Variability of Northern Pacific Storm Track during Winter①

Zhu Weijun (朱伟军), Sun Zhaobo (孙照渤)
Nanjing Institute of Meteorology, Nanjing 210044
Zhou Bing (周 兵)
LASG, Institute of Atmospheric Physics, Chinese Academy of Sciences, Beijing 100029

(Received September 1, 2000)

ABSTRACT

Investigation is conducted of the interannual variability of the northern Pacific storm track and its concurrent association with 500 hPa height and Pacific sea surface temperature (SST) during winter. Evidence suggests that during the studying period the center of the northern winter Pacific storm track experiences substantial interannual variability in the variation of its latitude, longitude and intensity. Singular value decomposition (SVD) of 15 winter 500 hPa filtered geopotential height variance over the storm track with the tropical and northern Pacific SST shows that the first coupled mode depicts the effect on the track of SSTA over the equatorial central and eastern Pacific, while the second one reflects the impact of Kuroshio SSTA on the track. Further Composite analysis indicates, moreover, that the SSTA over Kuroshio (equatorial central and eastern Pacific) during winter, which is relative to WP (PNA) teleconnection response pattern in 500 hPa height field, respectively, exerts crucial influence on the interannual variability in vigor and meridianal (zonal) displacement of the track over its central and western (eastern) part.

Key words: Storm track, Interannual variability, SVD analysis, Teleconnection pattern

1. Introduction

A storm track is an area in which the transient disturbance is extremely violent on the scale of 2.5–6 days. For the Northern Hemisphere there are two such significant areas, lying in the northern Pacific and Atlantic Oceans in middle latitudes, respectively. Since the discovery, with the aid of filtered data, of its existence in the end of the 1970's (e.g., Blackmon, 1976; Blackmon et al., 1977; Lau, 1979), research in the aspect has become an important branch in the field of 3–D transient wave dynamics. Progresses have been made in probing the mechanisms for maintaining the storm track and its internal dynamics (Hoskins and Valdes, 1990; Cai and Mak, 1990; Chang and Orlanski, 1993; Zhu and Sun, 1998; Sun and Zhu, 1998), though with little understanding so far of its interannual anomalies. As the condensation heating anomalies resulting from the transient disturbance over the track region pose important effect on global atmospheric circulation, and the heating itself directly brings forth changes in weather and climate, studying the anomalies and physical mechanism responsible for them is of essential importance for weather forecasting and short–term climate prediction. As is shown in some previous work, the vorticity flux caused by mid–latitude transient

①Sponsored by the China National Key Fundamental Research and Development Program (G1998040901–3) and National Natural Science Foundation of China (49475258).

disturbance during ENSO plays a vital role in maintaining the pattern of general atmospheric circulation over the northern Pacific and North America, which is triggered by the sea surface temperature anomaly (SSTA) over the equatorial region; the distribution of the flux itself is also subject to SSTA in the equatorial Pacific (Held et al., 1989; Hoerling and Ting, 1994; Straus and Shukla, 1997). Hoskins and Valdes (1990) pointed out that the warm western boundary currents of the oceans might also play an important role in maintaining the tracks during winter. As such, the aim of the current work is to use observed data to have a thorough discussion of the interannual anomalies and their possible physical mechanisms of the storm track in the northern Pacific in winter, from the point of external heating sources.

2. Data and methods

The current work uses the reanalyzed grid data for a global $2.5^\circ \times 2.5^\circ$ size in 1979–1994 from NCEP / NCAR and the global $1^\circ \times 1^\circ$ SST grid data in 1979–1994 compiled by the British Meteorological Office.

A 31-point digital band-pass filter, as introduced in Deng and Sun (1994), is first used here so that the transient eddies on a scale of 2.5–6 days are directly filtered out from the day-to-day original datasets. Then, the filtered data are divided into a section per winter month for which relevant variance is computed, and from which monthly mean band-pass filtered variance is thus derived. When conducting SVD analysis of the storm track (a filtered variance for the 500 hPa height) and the SST field, the length of every time series of grid data is set at 15 years, with the focus on standardized mean over the wintertime (from 1979 / 1980 to 1993 / 1994). Specifically, the winter mean refers to one over the five months from November and December of the preceding year down to January, February and March of the year that follows and represents the mean state of a given field in a given year. For the spatial domains, the value is selected over 100°E–100°W, 20°–70°N for the storm track in the northern Pacific and 105.5°E–78.5°W, 28.5°S–55.5°N for the SST in the Pacific.

Being one of the best methods for decomposing coupled patterns for any two fields, the SVD method is widely used in meteorology and it renders easy and illustrative usage, requiring no custom setting of parameters and hardly attaching any systematic error. Following Bertherton et al. (1992) and Wallace et al. (1992), we have studied the heterogeneous correlation patterns between different species.

3. Analysis of results

3.1 *The interannual variability of Northern winter Pacific storm track*

Before addressing the SVD results, let us take a look at the climatological position and vigor along with its interannual variability of the northern Pacific storm track, which are shown in Figs. 1 and 2, respectively. Following Blackmon (1976), Blackmon et al. (1977) and Lau (1979), the position and intensity of the storm track is expressed here by using the filtered variance of 500 hPa geopotential height. We can see from Fig. 1 that the maxima of 500 hPa filtered geopotential height variance are elongated along the whole mid-latitude Pacific Ocean, with its center lying at 172.5°E, 42.5°N, reaching as much as 40.4 dapgm^2 in magnitude, which is right the climatological position and vigor of the northern Pacific storm track. As considering its year-to-year variability, however, the center of the track experiences substantial variation in latitude, longitude and intensity. Figure 2 indicates that the vigor of the

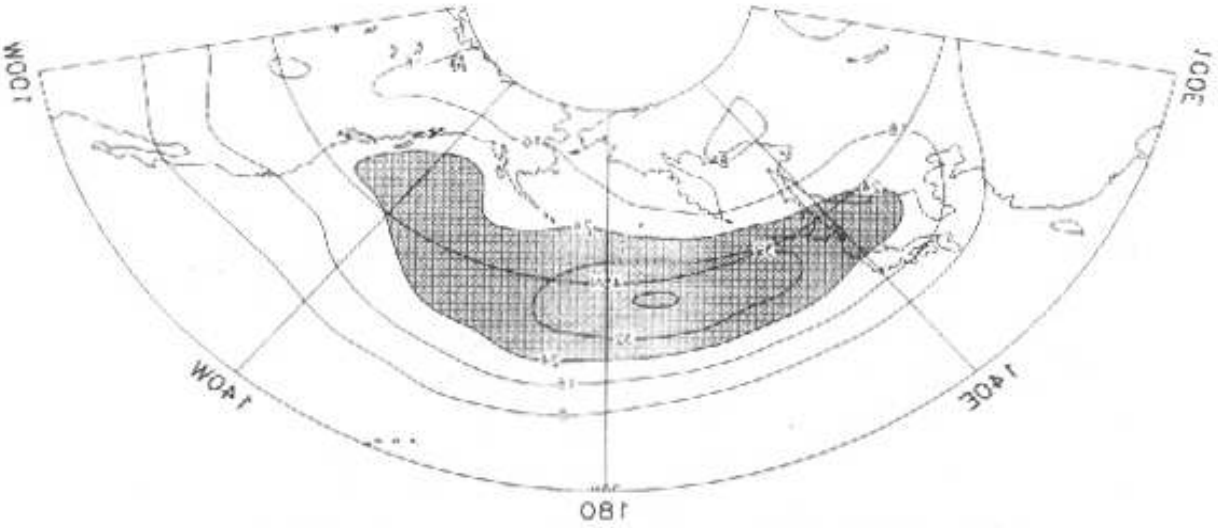

Fig. 1. The climatological northern Pacific storm track during winter. Contour interval: 8.0 dagpm^2.

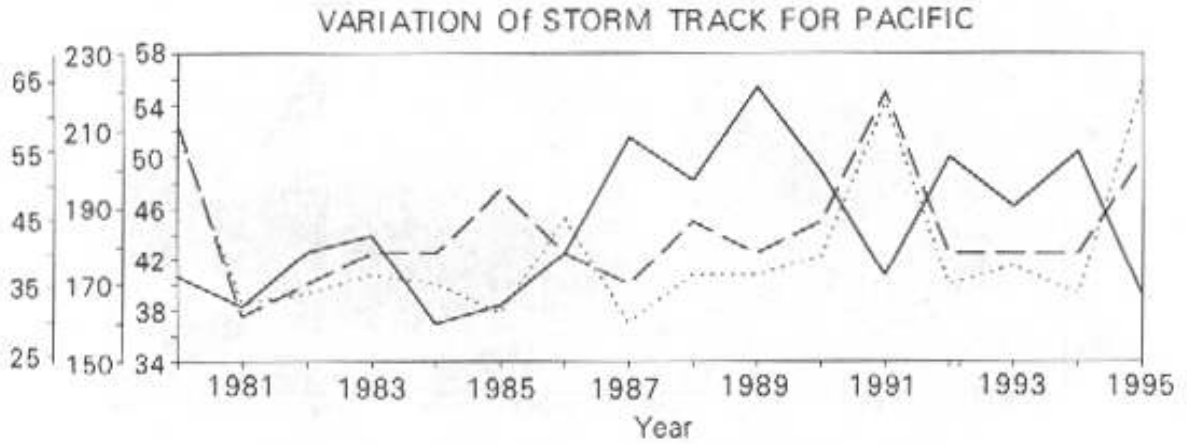

Fig. 2. Temporal variation in latitude (full), longitude (dashed) and intensity (dotted lines), respectively, of the track center. From left to right, the values in y-axis are for latitude (°N), longitude (°) and strength (dagpm^2), respectively.

track in the strongest year may vary twice as that in the weakest year, while its position in latitude and longitude may range from 30°–60°N and 160°E–100°W, respectively. Note that the center is here sought over the region of 100°E–100°W, 0°–90°N. The above result is in close agreement with that of Hu et al. (1997), who, on the basis of ECMWF objective analysis daily winds during 1980–1989, used the 300 hPa January mean kinetic energy to represent the winter mean position and vigor of the track.

3.2 *SVD results*

Figure 3 gives the first SVD mode (denoted by SVD1) of the winter 500 hPa geopotential height variance in the Pacific storm track and the Pacific SST along with the corresponding curve of temporal coefficients. As is described in Section 2, the eigenvectors are represented by the heterogeneous correlation patterns. For the filtered variance of the 500 hPa geopotential height (Fig. 3a), pattern SVD1 depicts how the storm track varies out of phase in

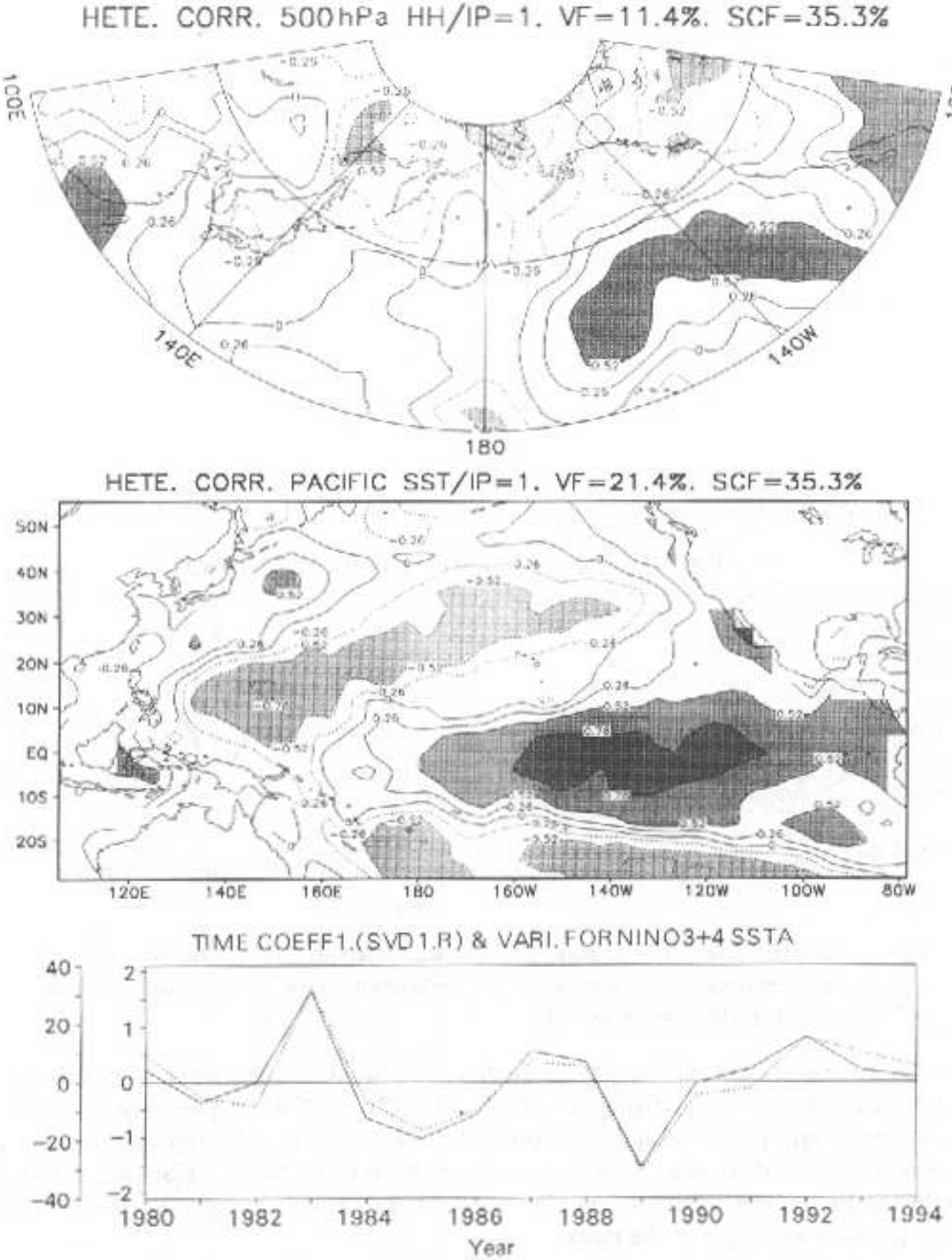

Fig. 3. Heterogeneous correlation patterns for the first SVD mode of the winter 500 hPa synoptic height variance in the Pacific storm track (a) and SST over the Pacific Ocean (b). The variance ratio explained by this mode is 35.3%, and the temporal correlation coefficient between the expansion coefficient of the two fields for the same mode is 0.92. Given in (c) is the temporal coefficients related to the SST field (dashed) and the SSTA series averaged over the Nino3+4 area (full line, in °C). Regions with correlation values above +0.52 and below −0.52 are shaded.

terms of intensity in areas north and south of 45°N in the mid-latitude central and eastern Pacific. Following the treatment introduced in Section 2, such pattern of variation is believed to reflect the interannual difference. For the Pacific SST (Fig. 3b), Pattern SVD1 shows the relationship of out-of-phase variation of concurrent SST between the equatorial central and eastern Pacific, the South China Sea and the northwestern Pacific and the remainder. The distribution bears high similarity to the transverse " V" pattern of SSTA during a typical ENSO episode. As a matter of fact, the three El Niño years (1982 / 1983, 1986 / 1987 and 1991 / 1992) and two La Niña years (1984 / 1985 and 1988 / 1989) in the period, as indicated by the dashe d curves of the temporal variation of the coefficients corresponding to Pattern SVD1 (Fig.3c), are clearly in opposite signs in temporal coefficients and all in their respective maximal values, implying that the SSTA in ENSO years has the largest contribution to such distribution pattern. The percentage of squared covariance that is interpreted by this pair of typical distribution pattern is 35.3% and the correlation coefficient is 0.92 between the two corresponding temporal coefficients, suggesting a high correlation in the pair. It is then clear that the interannual variation pattern of intensity and displacement in the middle and eastern sections of storm track over the northern Pacific in wintertime bears a close relation to the concurrent pattern of SST varying out-of-phase between the equatorial central and eastern Pacific, South China Sea and northwestern Pacific and the rest of the oceans.

Figure 4 gives the second SVD mode (denoted by SVD2) of the winter 500 hPa geopotential height variance in the Pacific storm track and the Pacific SST along with the corresponding curve of temporal coefficients. Again, the eigenvectors are represented by the heterogeneous correlation patterns. For the filtered variance of the 500 hPa geopotential height (Fig. 4a), pattern SVD2 depicts how the storm track varies out of phase in terms of intensity in areas of its climatological position and its north side with that to the south in the mid-latitude central and western Pacific. For the Pacific SST (Fig. 4b), Pattern SVD2 shows the out-of-phase variation of concurrent SST in the Kuroshio and equatorial central and eastern Pacific with the remainder. The variance ratio that is interpreted by this mode is 17.5% and the correlation coefficient is 0.92 between the two corresponding temporal coefficients, also suggesting a high correlation in the pair (Fig. 4c). It is therefore concluded that the interannual variation pattern of intensity and displacement in the middle and western sections of storm track over the northern Pacific in wintertime bears a close relation to the concurrent pattern of SST varying out-of-phase between the Kuroshio and equatorial central and eastern Pacific and the rest of the oceans.

Since the accumulative variance ratio interpreted by the above two modes is 52.8%, we would skip the discussion of the other SVD modes.

3.3 *Concurrent links to 500 hPa field in Northern Hemisphere*

By calculating the correlation between the temporal coefficient for the SST field of Patterns SVD1 and SVD2 and concurrent 500 hPa geopotential height in the Northern Hemisphere, respectively, we can get insight into links between the coupled patterns of SVD1 and SVD2 and the geopotential height field at 500 hPa in the hemisphere, respectively. As shown in Fig. 5, these distributions of correlation reflect that patterns SVD1 and SVD2 bear close relation to the PNA (Pacific and North America) and WP (Western Pacific) patterns at 500 hPa, respectively. Comparing Fig. 5 and Figs. 3 and 4, we also discover that the variation centers of the storm track in wintertime northern Pacific for Patterns SVD1 and SVD2 are right among the variation centers of the PNA and WP patterns, respectively. It is thus

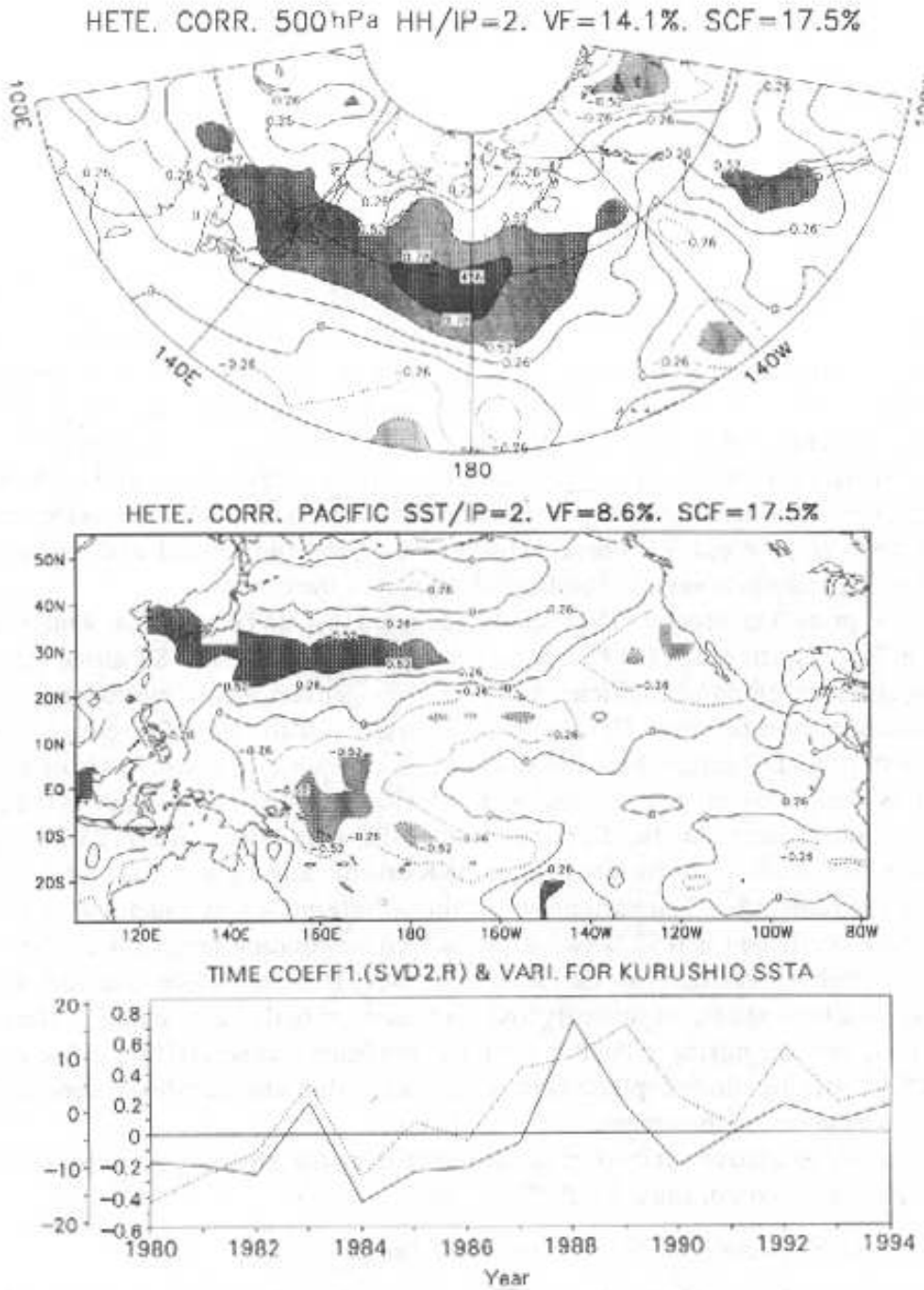

Fig. 4. Heterogeneous correlation patterns for the second SVD mode of the winter 500 hPa synoptic height variance in the Pacific storm track (a) and SST over the Pacific Ocean (b). The variance ratio explained by this mode is 17.5%, and the temporal correlation coefficient between the expansion coefficient of the two fields for the same mode is 0.91. Given in (c) is the temporal coefficients related to the SST field (dashed) and the SSTA series averaged over the Kuroshio area (full line, in °C). Regions with correlation values above +0.52 and below −0.52 are shaded.

concluded that the anomalous SST in the Pacific region in winter is closely related to concurrent changes in 500 hPa geopotential field and the storm track over the northern Pacific.

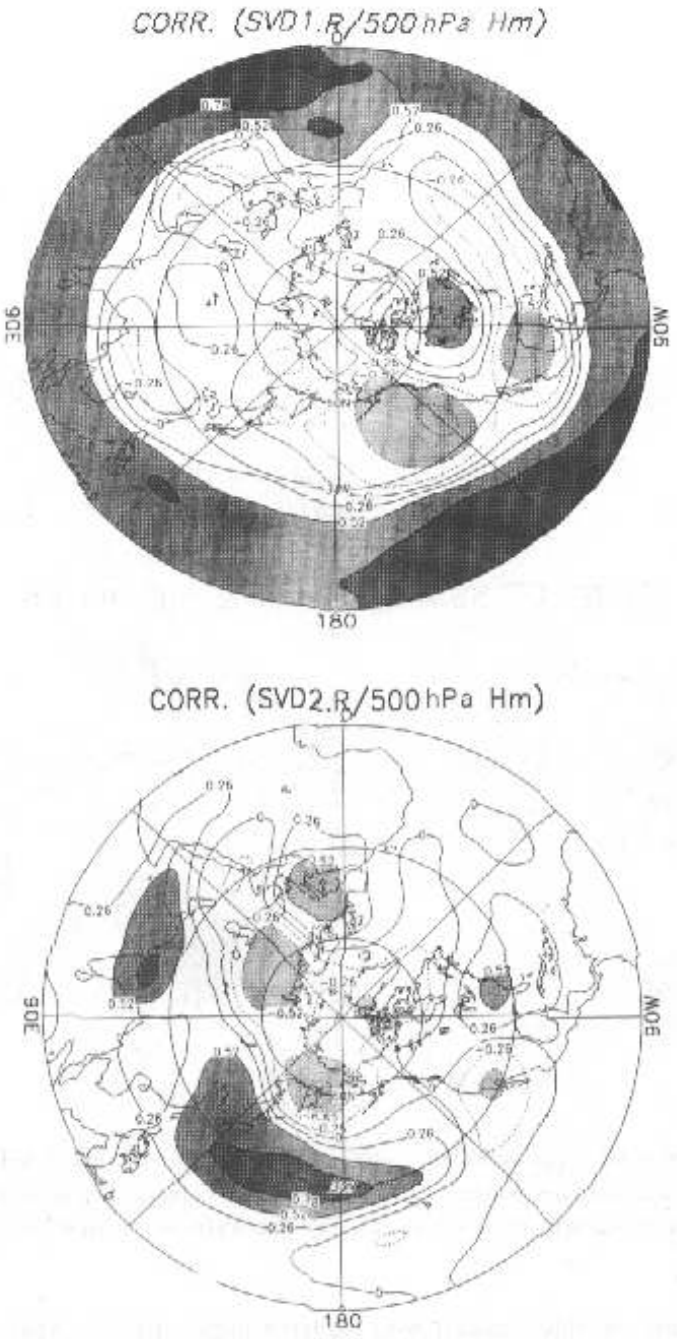

Fig. 5. Distributions of the correlation coefficients between the temporal coefficients of the SST for SVD1 (left) and SVD2 (right) and the monthly averaged 500 hPa height at individual grid points, respectively. Regions with correlation values above +0.52 and below −0.52 are shaded.

3.4 *Results of composite analysis*

Studying the SSTA distribution given in SVD1 and SVD2 patterns for the wintertime Pacific and its variation curves of temporal coefficients (Figs. 3b, c and Figs. 4b, c), we know that the equatorial central and eastern Pacific and Kuroshio area may turn out to be two

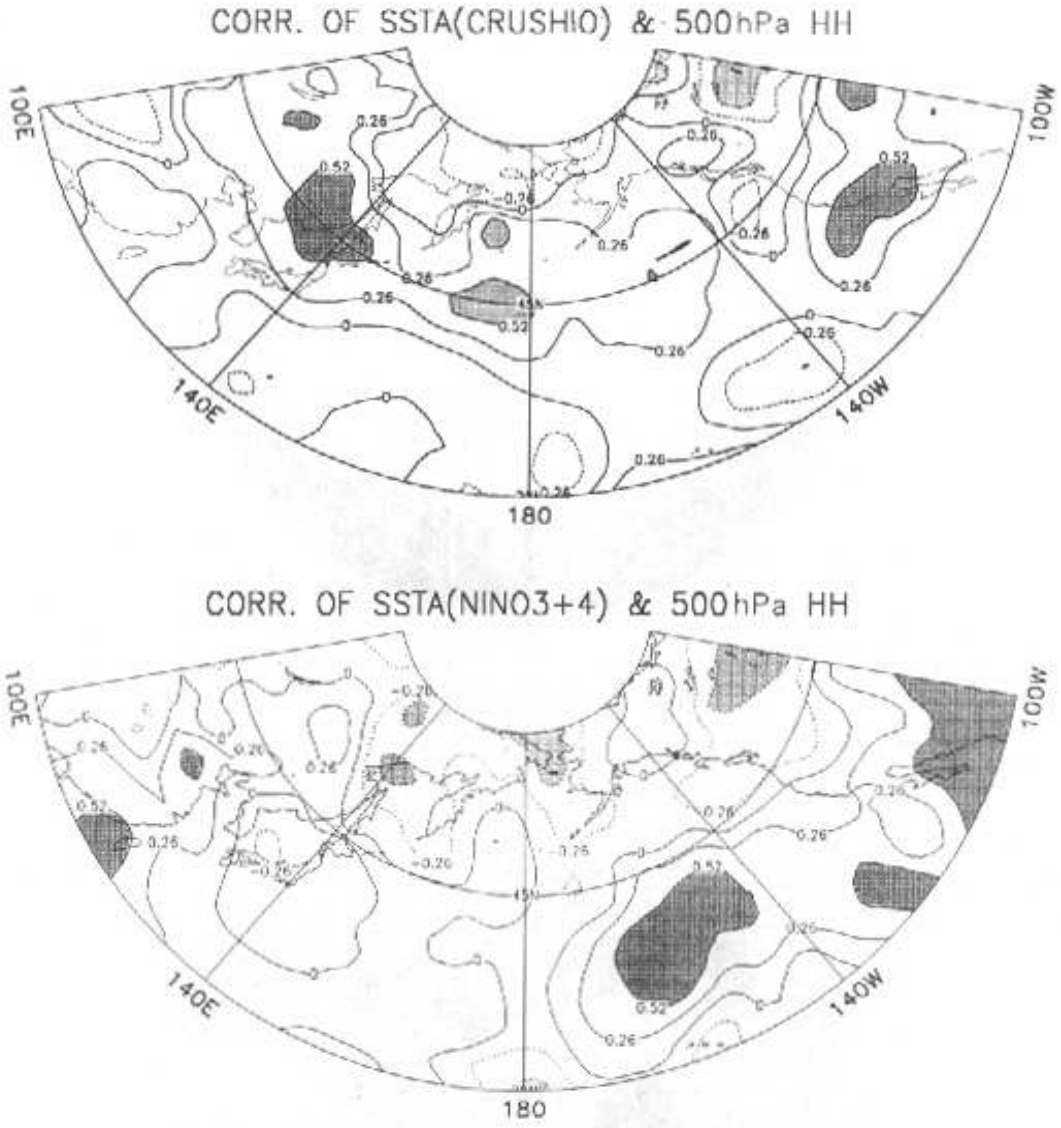

Fig. 6. Distributions of the correlation coefficients between the winter mean SSTA series over Nino3+4 (up) and Kuroshio (bottom) regions and the 500 hPa synoptic height variance at individual grid points, respectively. Areas with correlation values above +0.52 and below −0.52 are shaded.

signal zones. To confirm this presumption, we have highlighted the year–to–year curves of SSTA variations in Zones Nino 3+4 (160.5°E–90.5°W, 5.5°S–5.5°N, as indicated by the solid line in Fig. 3c) and Kuroshio (120.5°–150.5°E, 15.5°–32.5°N, the solid line in Fig. 4c). The figures present curves of SSTA variation over the zones that are very similar to that of the temporal coefficients for Patterns SVD1 and SVD2, respectively. The distribution of simultaneous correlation of this two SSTAs with the filtered variance of 500 hPa geopotential height and the height field itself are illustrated in Figs. 6 and 7, respectively. It can be seen from Fig. 6 that in wintertime Nino 3+4 (Kuroshio) the SSTA is correlated with the concurrent filtered variance of 500 hPa geopotential height by the most significant manner in the middle and eastern (western) regions of the Pacific storm track. The configurations are very close to the

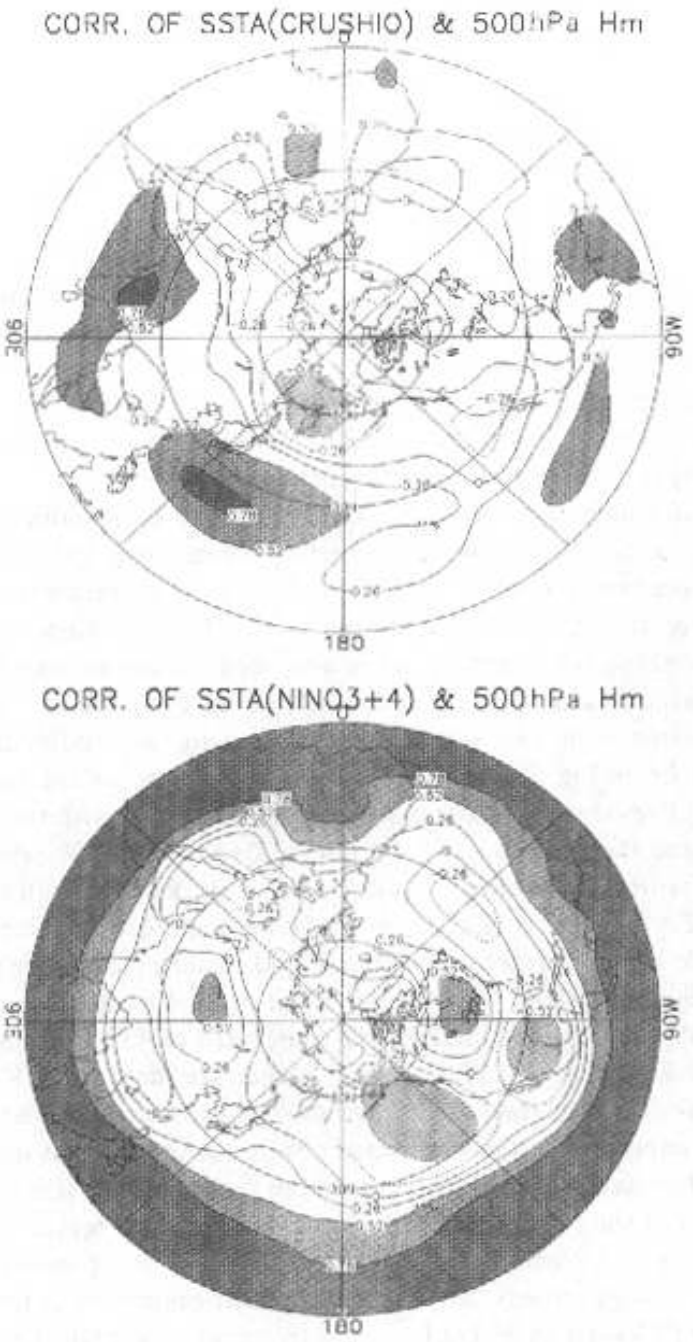

Fig. 7. Distributions of the correlation coefficients between the mean SSTA series over Nino3+4 (up) and Kuroshio (bottom) regions and the 500 hPa winter mean height field at individual grid points, respectively. Areas with correlation values above +0.52 and below −0.52 are shaded.

typical patterns of correlation distribution as given by Patterns SVD1 (Fig. 3a) and SVD2 (Fig. 4a), respectively. In addition, the same SSTAs are also in correlative distribution with the 500 hPa geopotential height field, which is given in Fig. 7. Results show relatively perfect PNA and WP teleconnection patterns almost identical to Figs. 5a, b, respectively. For this reason, we conclude that the results revealed by Patterns SVD1 and SVD2 are, in effect, reflecting the relationship between anomalous SSTs over the equatorial central and eastern Paci-

fic and Kuroshio in winter and concurrent anomalies of the Northern Pacific storm track and anomalous 500 hPa height, respectively.

It should be noted that the above results are only of correlation rather than of causality. On the other hand, both theoretic analysis and numerical simulation (e.g., Huang, 1991) have pointed to the possibility that the Pacific SSTA may trigger or strengthen the PNA and WP teleconnection patterns on the 500 hPa geopotential field so as to influence the changes in atmospheric circulation. And the storm track itself is in close relation to the jet stream over the same region (Deng and Sun, 1994). It is therefore reasonable to argue that the interannual variation of the storm track may be caused by such tele–response of the atmosphere to the ocean. One of the possibilities is that the wintertime SST anomaly in the Pacific may first influence the 500 hPa geopotential height field and then produces important effects on the concurrent interannual anomalies of the storm track in the northern Pacific. As a matter of fact, Held et al. (1989), Hoerling (1994) and Staus et al. (1997) have demonstrated that this relation might exist especially in a time when ENSO events happened.

In view of the consideration above, the months with absolute value of the SSTA $\geqslant 0.5$°C are selected from the zones Nino 3+4 and Kuroshio to composite Table 1 for further study of the effects of both positive and negative SSTAs there on the concurrent storm track for the northern Pacific. Figure 8 gives the distribution of the filter variance and difference of 500 hPa geopotential height in response to positive and negative anomalies of SSTA in Nino 3+4. To add to the conclusion more degree of reliability, we have conducted the t–test of difference significance for the mean of two samples. Regions with the confidence level larger than $\alpha = 0.05$ are shaded. From Fig. 8, we can see that for the equatorial central and eastern Pacific in winter, the north Pacific storm track is situated around 42°N with the bulk body extended towards southeast and the contour of 32 dagpm^2 shifted near 150°W when SSTA is positive. While the central position of the storm track remains little changed with the contour still west of 170°W when SSTA is negative. Relatively speaking, therefore, the intensity of disturbance on the synoptic scale is much larger in the middle and eastern part of the storm track in times of positive than negative SSTA, with the significance of difference reaching the level of $\alpha = 0.05$ away from the disturbance intensifying southward of 45°N. Figure 9 shows the same situation but for the Kuroshio area. From Fig. 9 we can see that for the Kuroshio area in winter, the northern Pacific storm track is situated more northward than the climate mean when SSTA is positive as composed to the southward position when SSTA is negative. Relatively sp eaking, therefore, the intensity of disturbance on the synoptic scale is much larger in the middle and western part of the storm track in times of positive than negative SSTA, with the significance of difference also reaching the level of $\alpha = 0.05$. By comparison of Fig. 3a and Fig. 8c, Fig. 4a and Fig. 9c, respectively, we find that the distributions of difference are much similar to the patterns of SVD1 and SVD2 for the filter variance at 500 hPa geopotential height, respectively.

The above results show that the positive SST in the equatorial central and eastern Pacific has important contribution to the eastward extension and consequent increase of the northern Pacific storm track in the middle and eastern sections while the negative SST causes a largely opposite situation. The result agrees well with the conclusion drawn in discussions of the role of ENSO events in maintaining the track (Zhu and Sun, 1998). In addition, Hu and Huang (1997) reported that the eastward extension of the storm track shows an obvious linear strengthening trend since the 1980's. It may, in our viewpoint, is related to higher frequency of ENSO outbreaks after the time.

Table 1. Years relative to SSTA above and below 0.5°C over Nino 3+4 and Kuroshio regions

	KUROSHIO AREA	NINO 3+4 AREA
+SSTA	1987 / 1988, 1993 / 1994	1982 / 1983, 1986 / 1987, 1991 / 1992
-SSTA	1981 / 1982, 1983 / 1984, 1989 / 1990	1984 / 1985, 1988 / 1989

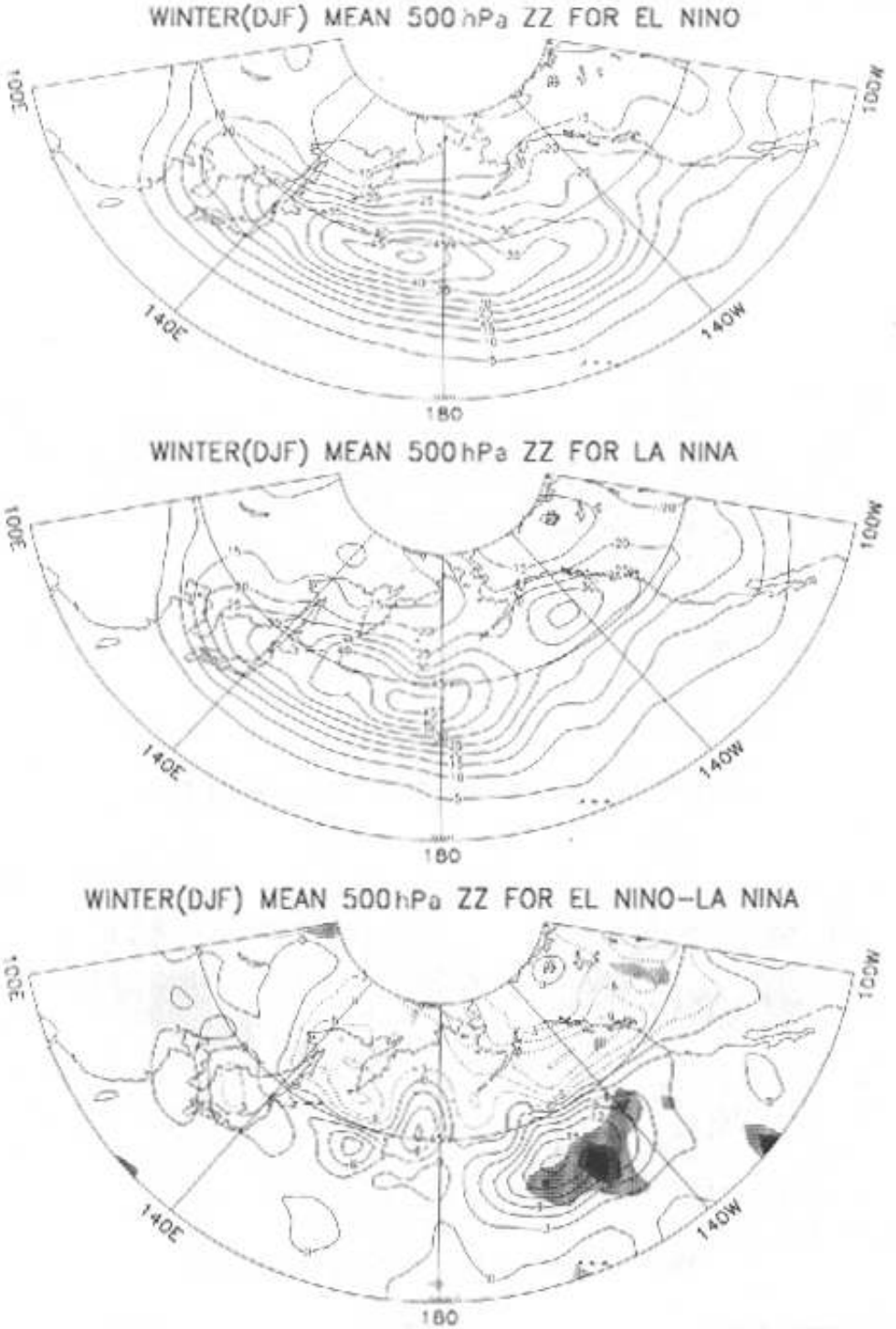

Fig. 8. Northern 500 hPa synoptic geopotential height variance composites for winter positive (a), negative (b) SSTA over the equatorial central and eastern Pacific area and their difference (c) with contour interval of 5.0 (a, b) and 3.0 (c) dagpm^2, respectively. Shaded areas in (c) indicate that passing t-test at $\alpha = 0.05$ confidence level.

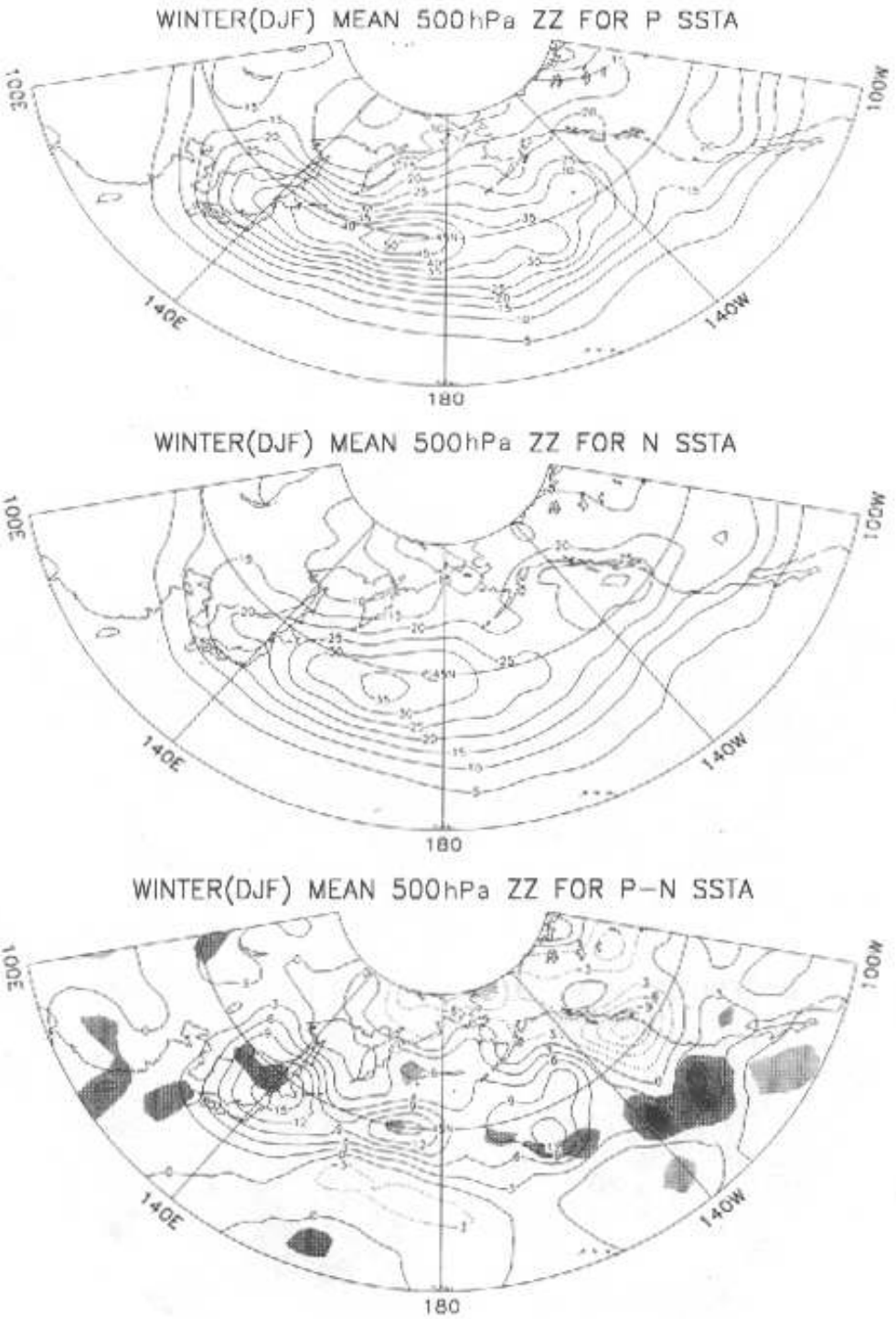

Fig. 9. The same as in Fig. 8 but for the Kuroshio area.

4. Concluding remarks

(1) The winter Pacific storm track experiences substantial interannual variation in latitude, longitude and intensity on a year-to-year basis. The vigor of the track in the strongest year may varies twice as that in the weakest year, while its position in lati-

tude and longitude may range from 30°–60°N and 160°E–100°W, respectively.

(2) The SVD1 pattern obtained from SVD analysis describes how the northern Pacific storm track varies out–of–phase in regions south and north of 45°N in mid–latitude central and eastern Pacific during winter, which is coupled with the concurrent variation of SSTA in the equatorial central and eastern Pacific. While the SVD2 pattern reflects how the northern Pacific storm track varies out–of–phase in regions south and north of its climate position in the mid–latitude central and western Pacific, during winter, which is coupled with the concurrent variation of SSTA in the Kuroshio area.

(3) The SVD1 and SVD2 patterns are closely linked with the PNA and WP patterns on the 500 hPa geopotential height field in Northern winter, respectively. It suggests that the wintertime SST anmalies in the Pacific may first influence the 500 hPa geopotential height field and then produces important effects on concurrent interannual anomalies of the storm track in the northern Pacific.

(4) More composite study shows that the wintertime anomalous SST in the equatorial central and eastern Pacific has important contribution to the east–west oscillation and changes in intensity of the storm track in the mid–latitude central and eastern Pacific. While the wintertime anomalous SST in the Kuroshio area is crucial for the north–south migration and changes in vigor of the track over the mid–latitude central and western Pacific.

It should be noted that apart from the external heat forcing chosen for the current work –SSTA in the Pacific in winter, there are other factors that the interannual variations of the northern Pacific storm track in winter are subject to. More study needs to be done to reveal their effects.

REFERENCES

Blackmon, M. L, 1976: A climatological spectral study of the 500 hPa geopotential height of the Northern Hemisphere. *J. Atmos. Sci.*, **33(8)**, 1607–1623.

Blackmon, M. L, J. M. Wallace, N. C., Lau et al., 1977: An observation study of the Northern Hemisphere wintertime circulation. *J. Atmos. Sci.*, **34(7)**, 1040–1053.

Bretherton, C. S., C. Smith, and J. M. Wallace, 1992: An intercomparison of methods for finding coupled patterns in climate data. *J. Climate*, **5**, 541–560.

Cai, M., and M. Mak, 1990: On the dynamics of regional cyclogenesis. *J. Atmos. Sci.*, **47(2)**, 1417–1442.

Chang, E. K., and M. I. Orlanski, 1993: On the dynamics of a storm tracks. *J. Atmos. Sci.*, **50(7)**, 999–1015.

Deng Xingxiu, and Sun Zhaobo, 1994: Features of temporal evolution of storm track in Northern Hemisphere. *J. Nanjing Inst. Meteov.*, **17(2)**, 165–170 (in Chinese).

Held, I. M., S. W. Lyons, and S. Nigam, 1989: Transients and the extratropical response to El Niño. *J. Atmos. Sci.*, **46(1)**, 163–174.

Hoerling, M. P., and M. Ting, 1994: Organization of extratropical transient during El Niño. *J. Climate*, **7**, 745–766.

Hoskins, B. J., and P. J. Valdes, 1990: On the existence of storm tracks. *J. Atmos. Sci.*, **47(15)**, 1854–1864.

Huang Ronghui, 1991: Teleconnections of atmospheric circulation. In: *Contemporary Study of Climate*, edited by Ye Duzheng et al. Beijing: China Meteorological Press, 113–136 (in Chinese).

Hu Zengzhen, and Huang Ronghui, 1997: The interannual variation of the convective activity in the tropical west Pacific in winter and its effect on the storm track in the north Pacific. *Scientia Atmospherica Sinica*, **21(5)**, 513–522 (in Chinese).

Lau, N. C., 1979: The structure and energetics of transient disturbance in the Northern Hemisphere wintertime circulation. *J. Atmos. Sci.*, **36(6)**, 982–995.

Straus, D. M., and J. Shukla, 1997: Variations of midlatitude transient dynamics associated with ENSO. *J. Atmos.*

Sci., **54(7)**, 777–790.

Sun Zhaobo, and Zhu Weijun, 1998: A possible mechanism for the maintenance of the Northern Hemisphere wintertime storm tracks. *J. Nanjing Inst. Meteor.*, **21(3)**, 299–306 (in Chinese).

Wallace, J. M., C. Smith, and C. S. Bretherton, 1992: Singular value decomposition of wintertime sea surface temperature and 500 mb height anomalies. *J. Climate*, **5**, 561–576.

Zhu Weijun, and Sun Zhaobo, 1998: ENSO effect on the maintenance of wintertime Pacific storm track. *J. Nanjing Inst. Meteor.*, **21(2)**, 189–195 (in Chinese).

冬季太平洋 SSTA 对北太平洋风暴轴年际变化的影响

朱伟军 孙照渤 周 兵

摘 要

研究了冬季北太平洋风暴轴的年际异常及其与 500hPa 高度以及热带和北太平洋海温的联系。结果发现，冬季北太平洋风暴轴中心有线性增强、偏北、偏东的趋势。对 15 个冬季北太平洋风暴轴区域 500 hPa 天气尺度滤波位势高度方差与同期热带和北太平洋海温的 SVD 分析表明，第一对空间典型分布反映了 ENSO 区海温异常对风暴轴年际变化的影响，而第二对空间典型分布反映了黑潮区域海温异常对风暴轴年际变化的影响。进一步的合成分析显示，ENSO 区海温异常可以通过激发 500hPa 高度场上的 PNA 遥相关型影响冬季北太平洋风暴轴的东西摆动和中、东端的强度变化，而黑潮区域海温异常则通过激发 500 hPa 高度场上的 WP 遥相关型，主要影响冬季北太平洋风暴轴中、西端的强度变化和南北位移。

关键词：风暴轴，年际变化，SVD 分析，遥相关型